Electrochemical Promotion by Potassium of Rhodium-Catalyzed Fischer−Tropsch Synthesis: XP Spectroscopy and Reaction Studies

Andrew J. Urquhart, James M. Keel, Federico J. Williams, and Richard M. Lambert*

Chemistry Department, Cambridge University, Cambridge, CB2 1EW, United Kingdom

Received: May 23, 2003; In Final Form: July 29, 2003

The catalytic behavior, chemical state, and morphology of a Rh thin film catalyst electrochemically promoted by alkali have been investigated by reactor studies, XPS, and SEM. At 1 bar pressure and 473 K, electropumped alkali decreases overall activity toward the production of hydrocarbons from CO and H_2 while increasing selectivity toward higher hydrocarbons, especially alkenes. On the active surface, rhodium is in a partially oxidized state; however, the catalytic activity is assigned to the metallic (Rh^0) component. The promoter phase is an alkali compound other than carbonate, although at high alkali loadings large amounts of crystalline alkali carbonate are deposited on the surface. The heavily carbonated system nevertheless retains most of its catalytic activity, with continued increase in selectivity toward higher hydrocarbons as the alkali loading is increased. Fully reversible behavior is found in every respect, including recovery of the initial state by electrochemical decomposition of the crystalline alkali carbonate deposit. The reaction mechanism is discussed with respect to the identity of the active site and the role of the alkali promoter.

Introduction

Electrochemical promotion (EP) is a strongly nonfaradaic phenomenon that combines heterogeneous catalysis with solid-state electrochemistry.[1,2] It enables controlled and reversible alteration of the behavior of thin film metal catalysts in contact with ionic conductors which act as electro-active supports from which mobile promoter species may be pumped to or from the catalyst surface under reaction conditions. It is this in situ tuning of catalytic behavior that makes EP unique. In the case of EP by alkalis, the underlying phenomena are rather well understood[3] so that EP combined with electron spectroscopy can provide a powerful means of elucidating catalytic mechanisms[4] for a wide variety of reactions, as exemplified by references 5−13.

Fischer−Tropsch synthesis (FTS), discovered eighty years ago, continues to attract attention for both academic and technical reasons. In this respect, the situation is not unlike that which prevails in regard to ammonia synthesis—an even older and simpler process for which increased fundamental understanding[14−16] and a consequent improvement in catalytic performance[15] have recently been achieved. FTS is the heterogeneously catalyzed synthesis of hydrocarbons and oxygenates from CO and H_2; a recent comprehensive review is provided in ref 17. Cobalt, iron, and ruthenium catalysts have been extensively investigated, where in each case alkali promotion results in a significant increase in selectivity toward higher hydrocarbons; Fe and Co catalysts are actually used technically (∼500−600 K/10−60 bar[18,19]). By comparison, Rh has been little studied. In this context, rhodium is particularly interesting because of its tendency to yield linear alcohols in addition to hydrocarbons.[20] Here we report the first application of EP and XPS to an investigation of alkali-promoted rhodium-catalyzed FTS at atmospheric pressure. The effects of alkali promotion on catalytic performance, the chemical state of the active surface, and the role of the promoter phase are elucidated. These results also provide the basis for understanding the system's behavior at much higher pressures.[21] Long ago, Brady and Pettit[22] demonstrated that adsorbed methylene is a key intermediate in FTS. Even so, the molecular mechanism remains controversial,[17] as does the mode of promoter action. Moreover, product speciation is seldom discussed (e.g., production of 1-alkenes versus 2-alkenes), and very little is known about the chemical state of the surface under reaction conditions. Here, we attempt to shed light on these issues.

Experimental Methods

Experiments were performed in a VSW ARIES system described elsewhere,[23] modified by addition of a flow-through reactor cell that could be operated at atmospheric pressure. After evacuation, sample transfer between the reactor cell and the analysis chamber allowed postreaction XPS analysis of the catalyst surface. Reaction gas consisting of H_2/CO 10:1 (BOC Gases) was delivered by means of electronic mass flow controllers at a total flow rate of 70 STP cm^3 min^{-1}. Reactor inlet and outlet gas analysis was carried out by means of a gas chromatograph (Shimadzu 14B) equipped with a FID and a DB-1 column (J&W Scientific). The reaction cell volume was 70 cm^3, and reactivity data were acquired at a pressure of 1 bar. After catalytic reaction measurements, the cell was evacuated by a turbo pump and the EP sample transferred to the UHV chamber (within ∼10 min) for XPS analysis. XP spectra were recorded using Mg Kα radiation with the Rh catalyst film at ground potential. Quoted binding energies are referenced to the Au $4f_{7/2}$ emission at 84 eV obtained from a gold wire which formed the electrical contact to the working electrode.

The EP sample consisted of a K-β'' alumina solid electrolyte wafer 12 × 18 × 2 mm (Ionotec Ltd., 99.99%) onto one side of which a thin rhodium film (5 μm) was sputtered—this was the working electrode—the catalytically active element. Catalytically inert gold reference and counter electrodes were sputter-deposited on the other side of the wafer—to provide a standard

* Corresponding author. Tel: 44 1223 336467. Fax: 44 1223 336362. E-mail: rml1@cam.ac.uk.

10.1021/jp035436q CCC: $25.00
Published on Web 08/29/2003

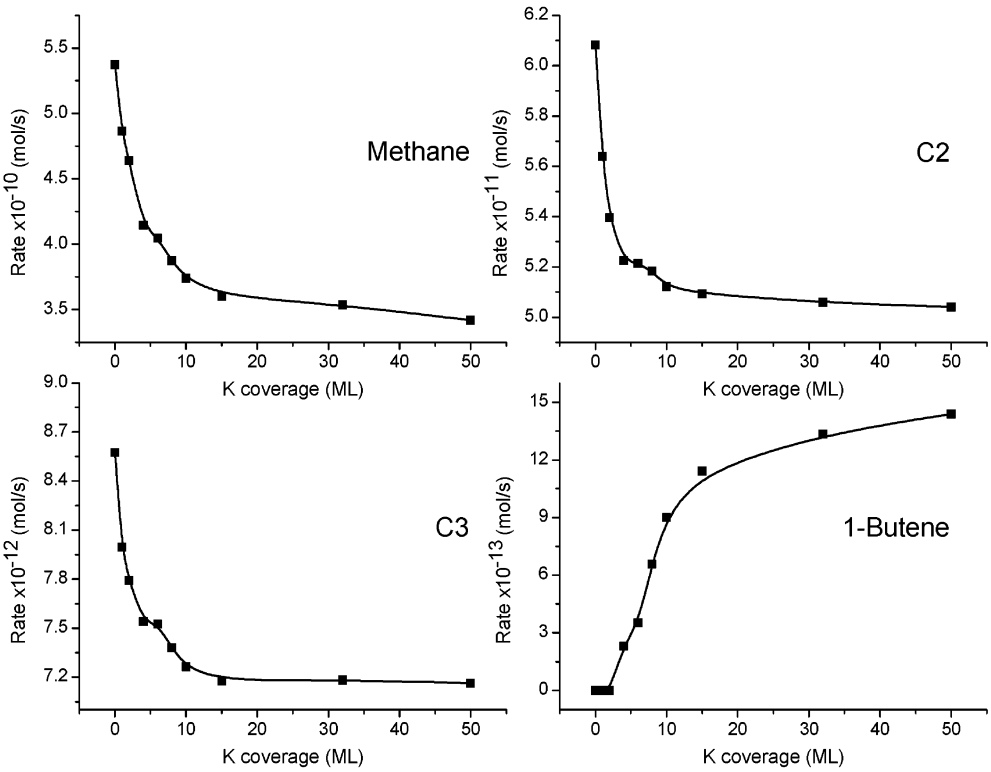

Figure 1. Rate of product formation as a function of K loading for reaction carried out over a rhodium thin film catalyst at 473 K, 1 bar, and with an inlet gas composition of CO/H_2 of 1:10.

3-electrode system for electrochemical control. The sample was mounted on an integrally heated machined ceramic block, and gold wires were used to make connections to the three electrodes. Electrochemical control of the sample was by means of a potentiostat−galvanostat (Ionic Systems, PG1). Ex-situ scanning electron microscopy (SEM) was performed with a JEOL 6340 FEG microscope operated at 20 kV; the surface area of the Rh film, estimated by CO methanation,[24,25] was 250 cm^2.

Results

The sample was cleaned by repeated cycles of heating in oxygen and hydrogen (30 min/550 K) until the XP spectrum showed only the presence of metallic Rh[26,27]($3d_{7/2}$ BE 307.0 eV). No Al, O or alkali signals were detectable. This demonstrates that the starting surface was indeed clean and that the underlying electrolyte was invisible to XPS. The latter observation is a reflection of the detection geometry; at near normal photoelectron exit angles, not accessible in our apparatus, the solid electrolyte is XPS-visible due to the presence of pores and cracks in the overlying metal film.[25,28]

Catalytic measurements were carried out at 473 K (typical for FTS) using a 10:1 H_2/CO ratio. A hydrogen-rich gas composition was used in order to minimize carbon deposition, which, as reported elsewhere,[21] becomes a significant problem with Rh at pressures above 1 bar. Controlled amounts of alkali were delivered to the sample galvanostatically, i.e., at constant current for a known time (∼100 μA), so that the absolute amount of alkali delivered to the sample may be readily calculated. Our earlier work demonstrated that the alkali promoter does indeed appear quantitatively at the surface of the catalyst[4,7,25] so that knowledge of the Rh surface area permits calculation of the nominal surface coverage of alkali, quoted here in monolayers (ML; 1 ML = 10^{15} alkali atoms/cm^2).

In passing, we note that in the present case alkali promotion under potentiostatic conditions (alkali pumped to/from the sample until a prescribed catalyst potential is reached) was not convenient. Large current transients occurred each time a new catalyst potential was specified—indicating extensive buildup of material on the catalyst surface, presumably due to rapid reaction between the electro-pumped alkali and the reactive gas atmosphere. As we shall see, such phenomena do indeed occur. Therefore, data were usually acquired under galvanostatic conditions which enable precise control of alkali transport and surface coverage.

Reactor Results. Figure 1 shows the effect of varying amounts of promoter (0−50 ML of alkali) on catalytic activity toward the formation of methane, C2 and C3 products, and 1-butene, the only C4 product. The data were acquired by starting with a clean Rh surface, and, under galvanostatic conditions, supplying successive increments of alkali to the catalyst under reaction conditions (10:1 H_2/CO, 473 K, 1 bar).

A steady-state reaction rate was established at each point (∼30 min) before carrying out product analysis. No higher hydrocarbons or oxygenates were detected—a situation that changes dramatically at higher pressures where EP measurements have to be carried out in another apparatus, as reported elsewhere.[21] (For C2, C3 products our GC column did not resolve alkenes and alkanes.) Note that a nominal loading of 50 ML alkali reduces C1, C2, C3 activity by 34%, 16%, and 16%, respectively; i.e., the catalyst is nowhere near fully poisoned, despite the very large amount of alkali that had been pumped to the surface. Note also the inflection that occurs in the C1, C2, C3 data at ∼5 ML and that this coincides with the onset of 1-butene production: un-promoted Rh produced no 1-butene under our conditions. Figure 2 shows the corresponding selectivity data derived from the results shown in Figure 1. It is evident that alkali promotion increases selectivity toward C2−C4 products

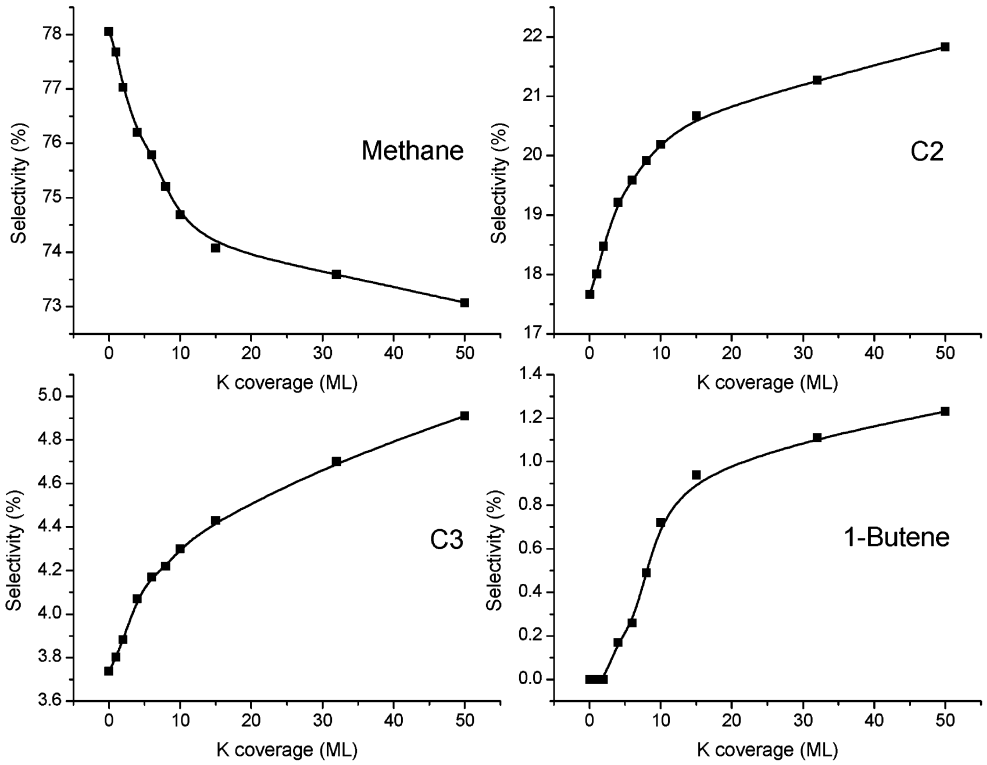

Figure 2. Product selectivity as a function of K loading for reaction carried out over a rhodium thin film catalyst at 473 K, 1 bar, and with an inlet gas composition of CO/H_2 of 1:10. Derived from data shown in Figure 1.

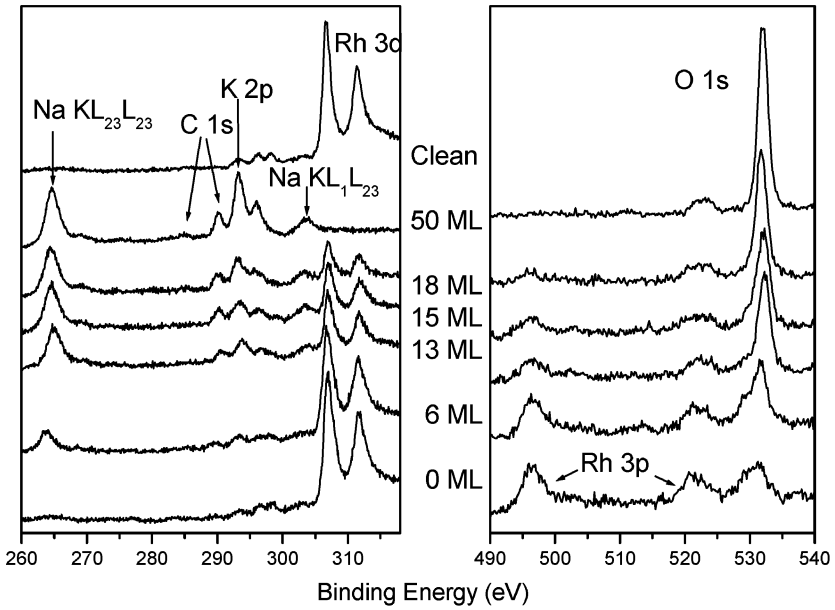

Figure 3. Pre- and postreaction XP spectra of the Rh 3d, K 2p, C 1s, and O 1s regions for the Rh thin film catalyst as a function of alkali loading supplied galvanostatically.

at the expense of methane production: in this sense the behavior is qualitatively similar to that reported for Ru thin film[29] and for poly crystalline cobalt[30] operated at atmospheric pressure.

X-ray Photoelectron Spectroscopy. Postreaction XP spectra as a function of alkali loading (0−50 ML) were obtained as follows. After recording catalytic performance at maximum alkali loading (50 ML), the sample was cooled, the reactor cell was evacuated, and the sample was transferred to the UHV spectrometer chamber. The corresponding XPS results are shown in the left and right panels of Figure 3; the top spectrum in the left panel of Figure 3 was taken with the pristine Rh catalyst before carrying out any promotion or reaction measurements. In addition to the strong Rh 3d doublet at 307.0 eV, charactersistic of *metallic rhodium*, small features are visible in the 296−299 eV range of binding energy (BE). These latter are the Rh 3d satellites due to the Mg $K\alpha_{3,4}$ X-radiation, necessarily present in the unfiltered source. In this 50 ML ex-reactor spectrum (left panel), all Rh 3d emission has been quenched, and C 1s peaks are apparent at 285 and 290.1 eV: these are assigned to surface carbon and a carbonate species respectively.[31−34] Note also the (expected) K 2p doublet at 292.9 eV and the presence of two Na KLL Auger transitions. Figure

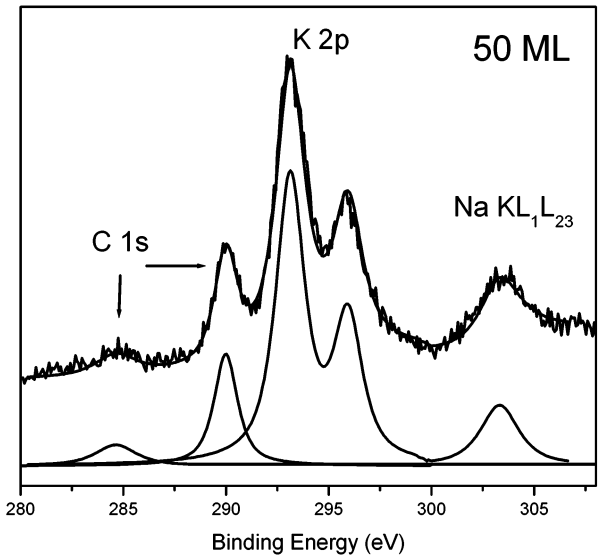

Figure 4. Curve-fitted postreaction XP spectrum of the K 2p and C 1s regions for the Rh thin film catalyst with a galvanostatically supplied alkali loading of 50 ML.

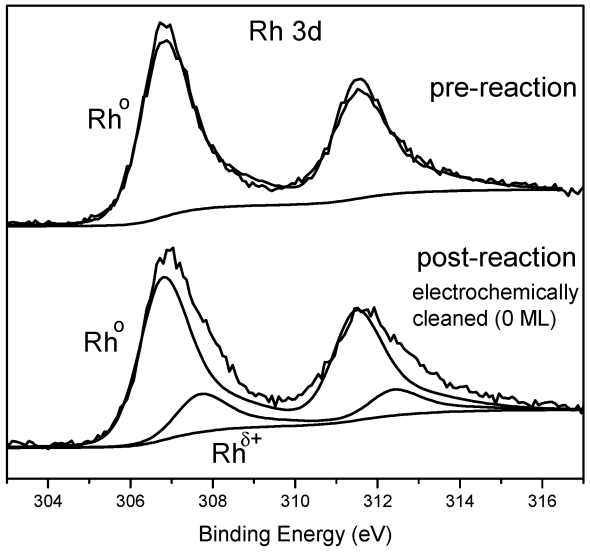

Figure 5. Pre- and postreaction curve-fitted XP spectra of the Rh 3d region for a Rh thin film catalyst.

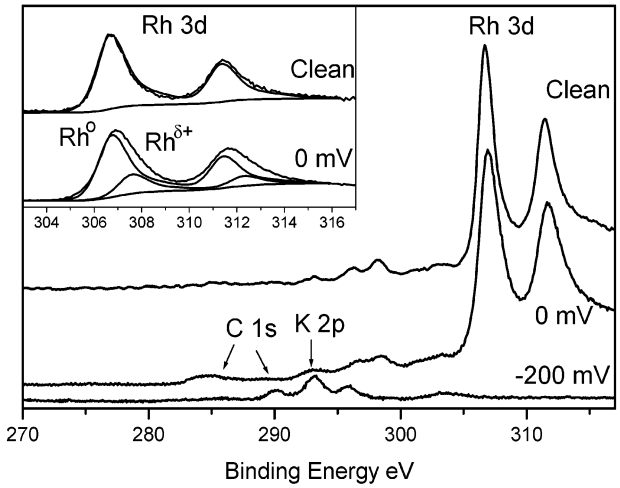

Figure 6. Pre- and postreaction XP spectra, of the Rh 3d, K 2p, and C 1s regions for the Rh thin film sample, as a function of catalyst potential (potentiostatic supply of alkali). Inset shows pre- and postreaction curve-fitted spectra for the Rh 3d region.

4 shows the 280−305 eV region in more detail. Assignment of the C 1s peak at 290.1 eV to carbonate is confirmed by the strong O 1s emission at 531.8 eV, a characteristic fingerprint of carbonate (right panel).[31,34] (The small feature at 520−525 eV is the O 1s satellite due to Mg K$\alpha_{3,4}$.)

Given that the K β'' alumina (made by molten salt ion exchange of Na β'' alumina) was assayed as 99.99% K, the presence of Na in the electro-pumped alkali may appear surprising. Taking account of photoionization cross sections, we calculate that the K/Na ratio at the surface was always ∼10:1. The implication is that the mobility of the residual (smaller) Na^+ ions in the solid electrolyte is much higher than that of the majority (larger) K^+ species. For present purposes, this is not critically important. It means that we are examining EP by a mixed alkali phase rather than by a pure K phase—and the literature shows that the promoting effects of Na and K in FTS are similar.[29]

After recording the 50 ML spectra, successive measured amounts of alkali were galvanostatically pumped away from the catalyst surface yielding the remaining spectra shown in both panels of Figure 3. At 18 ML the Rh emission reemerged and increased in intensity with increasing electro-pumping of alkali away from the surface; this was accompanied by a progressive decrease in the emission due to Na, K, and carbonate. Notice that the 0 ML spectrum (left panel) closely resembles the original "clean" spectrum, demonstrating the reversibility of electrochemical promotion—as the alkali ions are pumped back to the underlying solid electrolyte, the carbonate decomposes. Notice that this result also corresponds to the electrochemical recovery of a catalyst poisoned by over-promotion. In Figure 3, right panel, the 6 ML spectrum exhibits a shoulder at 530 eV. This feature which persists at 0 ML is ascribed to oxygen on rhodium. Notice the Rh 3p doublet which progressively increases in intensity as the surface is cleaned off.

By allowing for the various photoionization cross sections, we may use the 50 ML spectrum to quantify the relative amounts of alkali, carbon, and oxygen present within the XPS sampling depth (∼5 nm) with the following result: K/C/O = 4:1:3, which is potassium-rich relative to the 2:1:3 stoichiometry of potassium carbonate. However, for the 18, 15, and 13 ML cases, the estimated stoichiometry is ∼2:1:3—equivalent to potassium carbonate. The significance of this difference is discussed below. Finally, a close comparison of the Rh 3d lines from the pristine surface and from the 0 ML sample reveals the presence of a higher BE component in the latter case—upshifted by 0.7 eV with respect to the metallic Rh lines (Figure 5) signifying some degree of oxidation of the rhodium surface.

To check the validity of the "pump away" galvanostatic procedure used for post-reaction examination of the surface as a function of alkali loading, a limited number of potentiostatic experiments were carried out by pumping alkali to the catalyst in reaction gas at reaction temperature (Figure 6). Recall that this procedure gives relatively poor control of the amount of alkali delivered to the surface. The initial clean surface spectrum shows that the Rh film was metallic. Decreasing the catalyst potential to 0 mV under reaction conditions (which caused alkali to be pumped to the catalyst) broadened the Rh 3d doublet (see inset) demonstrating partial oxidation of the rhodium in the reactions gas. The K 2p, C 1s, and O 1s emissions correspond to those observed in the galvanostatic experiments. Decreasing the catalyst potential still further to −200 mV resulted in heavy

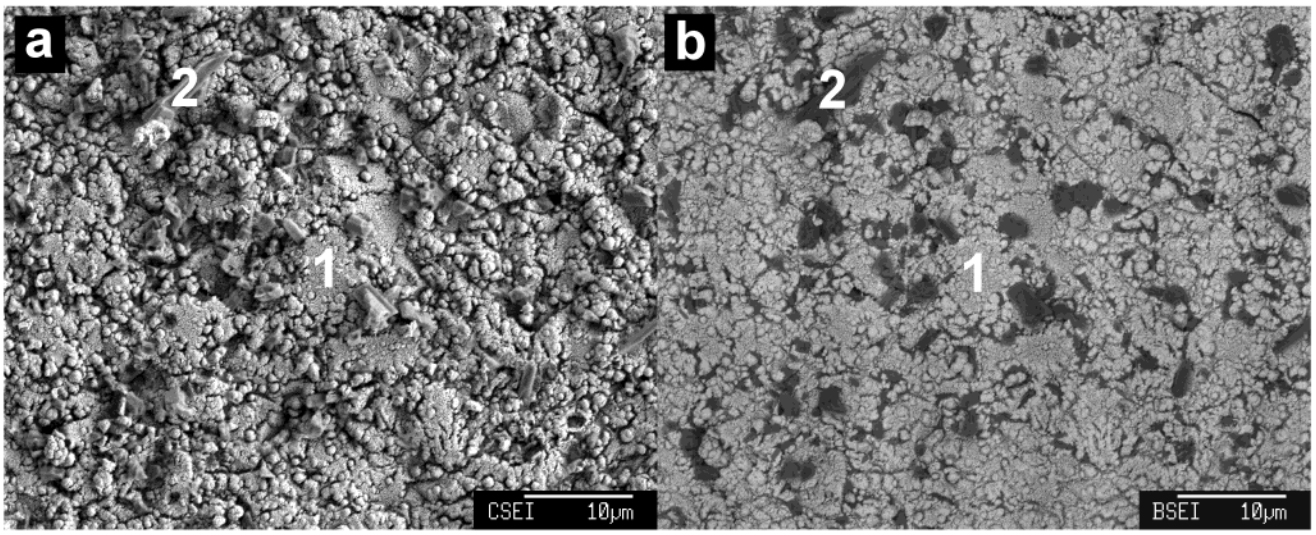

Figure 7. SEM images of postreaction rhodium thin film catalyst (a) secondary electron image, (b) backscattered electron image.

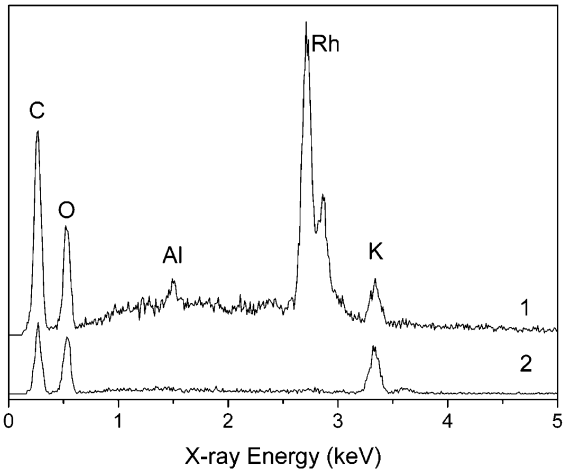

Figure 8. EDX spectra of postreaction rhodium thin film catalyst from positions labeled 1,2 in Figure 7.

accumulation of material on the catalyst, completely attenuating the Rh signal. As in the galvanostatic experiments, the system behaved reversibly. These results show that the chemical state of the catalyst is very similar in the two cases: galvanostatic *pumping away* of alkali after loading up in reaction gas has the same essentially effect as potentiostatic *pumping to* the initially clean surface in the presence of reaction gas.

SEM Results. Ex situ SEM images obtained from the postreactor 50 ML loaded sample are presented in Figure 7, and the corresponding EDX spectra are shown in Figure 8. The secondary electron image provides topographical information (Figure 7 a), while the backscattered electron mode (Figure 7 b) provides contrast dependent on atomic number: low atomic number dark, high atomic number bright. These measurements help us to understand how such high loadings of alkali did not suppress all catalytic activity. Inspection of Figure 7a,b indicates the presence of two different types of material, and EDX spectra taken from regions 1,2 are shown in Figure 8, regions 1,2. Keeping in mind that EDX, unlike XPS, is qualitative and not a surface-sensitive technique, it is clear that region 1 is rhodium-rich with a small amount of potassium. On the other hand, region 2 consists essentially of K, C, and O—presumably corresponding to the alkali carbonate whose presence was suggested by XPS. Moreover, the material in region 2 was very unstable in the electron beam, consistent with it being an alkali carbonate.

Discussion

The only products observed under our conditions were C1−C4 hydrocarbons; no higher hydrocarbons or oxygenates were detected. This may be attributed to the relatively low pressure—constrained to 1 bar due to apparatus limitations. (At pressures above 8 bar, electrochemically promoted Rh *does* catalyze the formation of both higher hydrocarbons and oxygenates.[21]) The principal effects of alkali promotion are to decrease all reaction rates and increase selectivity toward higher hydrocarbons at the expense of methane production—the most hydrogen-intensive reaction of all. It is also noteworthy that 1-butene rather than butane is produced, even though the gas composition is hydrogen-rich. We need to understand the nature of the catalytically active phase, the role of the alkali promoter, and the inflection in reaction rates that occurs at ∼5 ML alkali promoter.

Much has been written about the mechanism of FTS,[17] although much still remains to be clarified, partly as a result of incomplete or missing experimental information. For example, many authors do not report speciation of products, which are simply lumped together as "C_n" without reference to isomer content. Equally, in the majority of cases, little or nothing is known about the oxidation state of the catalytic metal under reaction conditions. The generally accepted mechanism[35] for FTS involves the following:

(i) CO dissociation,

(ii) hydrogenation of the resulting C adatoms to CH_2,

(iii) polymerization of CH_2 to from adsorbed alkyl species,

(iv) β-hydrogen elimination or hydrogen addition to form α-olefins or *n*-alkanes, respectively.

Maitlis and co-workers[36] have questioned the validity of this scheme, preferring a very different one in which the chemistry is triggered by reaction between CH(a) and CH_2(a) and β-hydrogen elimination is not invoked to account for the formation of α-olefins. But the first and critically important step is unsupported by direct evidence. Moreover, recent experimental results[37] contradict the Maitlis scheme. Accordingly, we shall adopt the generally accepted model as a working hypothesis.

It is well-known that adsorbed alkali weakens the C−O bond strength in carbon monoxide chemisorbed on transition metal surfaces.[38] However, there is good support for the view that step (i) is not rate-limiting (see ref 29 and references therein)

so that another reason must be sought for the effect of alkali. To elucidate the mechanism of promotion, we need to understand the morphology, distribution, and chemical state of the various species present on the active surface.

The XPS results (Figure 3) show that the decrease in overall activity caused by increased alkali loading may be ascribed to progressive blocking of active sites by some alkali compound—probably a carbonate. They also demonstrate that this material is not distributed uniformly across the metal surface. Thus Figure 3 shows that Rh 3d emission is still visible at a nominal coverage equivalent to 18 ML of alkali compound whereas, given the Rh 3d photoelectron mean free path, a uniform layer would result in complete extinction of the Rh lines at a coverage of ~4 nm, which corresponds to a loading of ~10 ML. The implication is that at high loadings most of the alkali carbonate is present as three-dimensional crystallites, leaving patches of nominally bare Rh on which the FTS reaction occurs. This conclusion is qualitatively consistent with the SEM and EDX results. Of course, the "bare" Rh patches cannot really be totally denuded of alkali compounds—else there would be no effect on the FTS selectivity.

Quantitative and qualitative estimates based on the XPS, SEM, and EDX data provide useful information about the nature of the active catalyst. Consider the 50 ML sample. SEM and EDX clearly show the presence of a large amount of micron-size crystallites, almost certainly alkali carbonate. Since we know the Rh surface area (~250 cm^2) and the amount of alkali supplied (50 ML), a straightforward calculation shows the amount of alkali pumped to the surface would correspond to enough material to produce a 4 nm layer (thus completely attenuating the Rh 3d signal) and then grow micron scale crystallites of alkali carbonate in the size range observed by SEM. The O 1s BE observed by XPS corresponds well with an alkali carbonate. The 50 ML XPS intensity ratios are potassium-rich compared to K_2CO_3. Given the sampling depth of XPS, it follows that a very large proportion of the carbonate is XPS-invisible. This fact, and the 4:1:3 K/C/O ratio estimated form XPS points to the presence of a significant amount of well dispersed K in some chemical state other than carbonate. We conjecture that this material is the promoter phase on the active metal surface. Support for this view derives from the fact that subsequent galvanostatic pumping of alkali away from the 50 ML ex-reactor sample down to a level of 18 ML (Figure 3) gave a K/C/O ratio of ~2:3:1, close to that of K_2CO_3. A plausible interpretation is as follows. Within the sampling depth of XPS, electro-pumping immediately depletes the 2D alkali promoter phase adsorbed on the Rh. In contrast, the spectral intensities due to the large 3D carbonate crystallites attenuates far more slowly. As a result, the 18 ML spectrum exhibits intensities dominated by K_2CO_3. How are we to account for the fact that the 50 ML sample is still catalytically active, even though no Rh emission is visible? The SEM data provides the answer. The surface is so heavily decorated by a very rough deposit of carbonate that any emerging Rh photoelectrons (~900 eV kinetic energy) are very strongly inelastically scattered before being detected; molecules can get in and out to/from the Rh surface; photons can get in, just; but emerging electrons experience overwhelming inelastic scattering.

A comparison of the spectroscopic (Figure 3) and reactor data (Figure 1) at ~5 ML, which corresponds to the inflection point in the rates of formation of all products is revealing. As a function of alkali loading, the rates of C1−C3 production fall into two distinct regimes. Up to ~5 ML, all three rates fall sharply; after the inflection point, they fall much more slowly. At this stage, the Rh 3d intensity has been attenuated by 10% with respect to the clean surface value. This behavior may be rationalized as follows: (i) up to ~5 ML loading, initial 2D growth of a promoting alkali compound on the Rh surface, altering catalytic selectivity at the same time attenuating activity by site blocking; (ii) at the ~5 ML inflection point, nucleation of 3D crystallites of alkali carbonate; (iii) subsequent growth of these 3D crystallites. As a result, after ~10 ML, continued electro-pumping of alkali has much less effect on activity and selectivity as most of the alkali supplied is now stored in the 3D crystallites of carbonate.

How is the alkali carbonate formed? It seems plausible[39] that alkali-induced CO dissociation triggers the process. A possible set of processes involving surface species could then be

$$CO \rightarrow C + O \quad \textit{alkali-induced}$$

$$2K + 2O \rightarrow K_2O_2$$

$$K_2O_2 + CO \rightarrow K_2CO_3$$

The peroxide rather than the normal oxide is written in the second step because we are under strongly reducing conditions.[40] From a mechanistic point of view, the issue of the oxidation state of the active metal catalyst is an important one and, in general, little or nothing is known about this. In the case of Fe catalysts, Lox et al.[41] concluded that both Fe and Fe_3O_4 are present. These results have been used to propose a bifunctional mechanism where the Fe_3O_4 component catalyzes the water gas shift reaction while the Fe component is responsible for FTS.[17] Our XP spectra indicate that the Rh surface is partially oxidized under reaction conditions. However, the BE upshift of the oxidic component is in the order of only 0.7 eV, compared to 1.2 eV which would correspond to Rh_2O_3.[26,27] Therefore we may conclude that the oxidized Rh component is in a lower oxidation state: +1 or +2 (no literature data is available). It is known that Rh_2O_3 is effective as a water gas shift catalyst. However, lower oxides of Rh are not.[42] Therefore, the remaining question is whether oxidized Rh is likely to be an effective FTS catalyst. If, as seems likely, the reaction-initiating step is CO dissociation,[39] then Rh^0 rather than $Rh^{\delta+}$ would certainly be the most effective reaction site; our tentative conclusion is that the oxidized Rh sites are not likely to be of importance in FTS.

The reactor results suggest that the promoter acts by inhibiting hydrogenation reactions relative to C−C bond formation, thus favoring chain growth. The promoter also favors alkene production, suggesting that it assists β-hydrogen elimination. Both effects may be qualitatively understood if the promoter somehow binds H_a more strongly than does the unpromoted Rh surface—the energetics of hydrogenation and β elimination would be disfavored and favored, respectively. The results indicate rather clearly that the promoter phase is something other than alkali carbonate, although on the basis of the present evidence we cannot determine exactly what it is. It is known that when H_a is coadsorbed with alkali, the hydrogen becomes more strongly bound to the surface,[42,43] possibly as the result of an adsorbed alkali hydride being formed. If such material is formed under the strongly reducing conditions used here, it would provide a basis for rationalizing the observed effects of alkali promotion. Further work is required to establish the precise chemical identity of the alkali promoter phase.

Conclusions

1. In Rh-catalyzed FTS, electro-pumped alkali decreases overall activity while promoting chain growth and the production of alkenes.

2. Rhodium in the catalytically active surface is in a partially oxidized state, however the catalytic activity is assigned to the metallic component.

3. The promoter phase is an alkali compound other than carbonate.

4. At very high alkali loadings, large amounts of crystalline alkali carbonate are deposited on the surface. Even so, the system retains most of its catalytic activity with continued increase in selectivity toward higher hydrocarbons. This carbonate phase can be decomposed electrochemically to recover the original behavior.

Acknowledgment. A.J.U. acknowledges the award of a research studentship by the UK Engineering and Physical Sciences Research Council and additional support from the Isaac Newton Trust. F.J.W. holds a Cambridge University Oppenheimer Fellowship.

References and Notes

(1) Vayenas, C. G.; Bebelis, S. *Catal. Today* **1999**, *51* (3−4), 581.
(2) Foti, G.; Bolzonella, I.; Eaves, J.; Comninellis, C. *Chimia* **2002**, *56* (4), 137.
(3) Lambert, R. M.; Williams, F. J.; Palermo, A.; Tikhov, M. S. *Top. Catal*. **2000**, *13* (1−2), 91.
(4) Williams, F. J.; Palermo, A.; Tracey, S.; Tikhov, M. S.; Lambert, R. M. *J. Phys. Chem. B* **2002**, *106* (22), 5668.
(5) Yentekakis, I. V.; Palermo, A.; Filkin, N. C.; Tikhov, M. S.; Lambert, R. M. *J. Phys. Chem. B* **1997**, *101* (19), 3759.
(6) Williams, F. J.; Palermo, A.; Tikhov, M. S.; Lambert, R. M. *J. Phys. Chem. B* **1999**, *103* (45), 9960.
(7) Williams, F. J.; Palermo, A.; Tikhov, M. S.; Lambert, R. M. *J. Phys. Chem. B* **2000**, *104* (3), 615.
(8) Tracey, S.; Palermo, A.; Vazquez, J. P. H.; Lambert, R. M. *J. Catal*. **1998**, *179* (1), 231.
(9) Williams, F. J.; Palermo, A.; Tracey, S.; Tikhov, M. S.; Lambert, R. M. *J. Phys. Chem. B* **2002**, *106* (22), 5668.
(10) Williams, F. J.; Palermo, A.; Lambert, R. M. *J. Phys. Chem. B* **2002**, *106* (39), 10215.
(11) Palermo, A.; Husain, A.; Tikhov, M. S.; Lambert, R. M. *J. Catal*. **2002**, *207* (2), 331.
(12) Karavasilis, C.; Bebelis, S.; Vayenas, C. G. *J. Catal*. **1996**, *160* (2), 190.
(13) Karavasilis, C.; Bebelis, S.; Vayenas, C. G. *J. Catal*. **1996**, *160* (2), 205.
(14) Nørskov, J. K.; Bligaard, T.; Logadottir, A.; Bahn, S.; Hansen, L. B.; Bollinger, M.; Bengaard, H.; Hammer, B.; Sljivancanin, Z.; Mavrikakis, M.; Xu, Y.; Dahl, S.; Jacobsen, C. J. H. *J. Catal*. **2002**, *209*, 275.
(15) Jacobsen, C. J. H.; Dahl, S.; Clausen, B. S.; Bahn, S.; Logadottir, A.; Nørskov, J. K. *J. Am. Chem. Soc*. **2001**, *209*, 275.
(16) Jacobsen, C. J. H.; Dahl, S.; Clausen, B. S.; Bahn, S.; Logadottir, A.; Nørskov, J. K. *Appl. Catal. A* **2001**, *222*, 19.
(17) Van der Laan, G. P.; Beenackers, A. A. C. M. *Catal. Rev. Sci. Eng*. **1999**, *255*, 41.
(18) Jager, B: Espinoza, R. *Catal. Today* **1995**, *23*, 17.
(19) Sie, S. T. *Rev. Chem. Eng*. **1998**, *14*, 109.
(20) Quyoum, R.; Berdini, V.; Turner, M. L.; Long, H. C.; Maitlis, P. M. *J. Catal*. **1997**, *173*, 355.
(21) Urquhart, A. J.; Williams, F. J.; Keel, J. M.; Lambert, R. M. In preparation.
(22) Brady, R. C.; Pettit, R. *J. Am. Chem. Soc.* **1980**, *102*, 6181.
(23) Horton, J. H.; Moggridge, G. D.; Ormerod, R. M.; Kolobov, A. V.; Lambert, R. M. *Thin Solid Films* **1994**, *237*, 134.
(24) Komai, S.; Hattori, T.; Murakami, Y. *J. Catal*. **1989**, *120*, 370.
(25) Williams, F. J.; Palermo, A.; Tikhov, M. S.; Lambert, R. M. *J. Phys. Chem. B* **2000**, *104* (50), 11883.
(26) Wagner, C. D.; Riggs, W. M.; Davies, L. E.; Moulder, J. F. *Handbook of X-ray Photoelectron Spectroscopy*; Muilenberg, G. E., Ed.; Perkin and Elmer Corporation, 1978; p 188.
(27) Suhonen, S.; Polvinen, R.; Valden, M.; Kallinen, K.; Härkönen, M. *Appl. Surf. Sci*. **2002**, *200*, 48.
(28) Yentekakis, I. V.; Palermo, A.; Filkin, N. C.; Tikhov, M. S.; Lambert, R. M. *J. Phys. Chem. B* **1997**, *101*, 3759.
(29) Williams, F. J.; Lambert, R. M. *Catal. Lett.* **2000**, *70* (1−2), 9.
(30) Lahtinen, J.; Somorjai, G. A. *J. Mol. Catal. A-Chem*. **1998**, *130* (3), 255.
(31) Williams, F. J.; Palermo, A.; Tikhov, M. S.; Lambert, R. M. *J. Phys. Chem. B* **2001**, *105* (7), 1381.
(32) Meyer, G.; Reinhart, E.; Borgmann, D.; Wedler, G. *Surf. Sci*. **1994**, *320*, 110.
(33) Meyer, G.; Borgmann, D.; Wedler, G. *Surf. Sci*. **1994**, *320*, 123.
(34) Filkin, N. C.; Tikhov, M. S.; Palermo, A. P.; Lambert, R. M. *J. Phys. Chem. A* **1999**, *103* (15), 2680.
(35) Iglesia, E. *Appl. Catal. A: General* **1997**, *161*, 59.
(36) Maitlis, P. M.; Quyoum, R.; Long, H. C.; Turner, M. L. *Appl. Catal. A* **1999**, *186*, 363.
(37) Ndlovu, S. B.; Phala, N. S.; Hearshaw-Timme, M.; Beagly, P.; Moss, J. R.; Claeys, M.; van Steen, E. *Catal. Today* **2002**, *71* (4), 343.
(38) Kiss, J.; Klivényi, G.; Révész, K.; Solymosi, F. *Surf. Sci*. **1987**, *223*, 551.
(39) Crowell, J. E.; Tysoe, W. T.; Somorjai, G. A. *J. Phys. Chem*. **1985**, *89*, 1598.
(40) Greenwood, N. N.; Earnshaw, A. *Chemistry of the Elements*; Pergamon: Oxford, 1986; Chapter 4.
(41) Lox, E. S.; Marin, G. B.; Degrave, E.; Bussiere, P. *Appl. Catal. A* **1988**, *40* (1−2), 197.
(42) Gebbard, S. C.; Koel, B. E. *J. Phys. Chem*. **1992**, *96*, 7056.
(43) Zhou, X. L.; White, J. M. *Surf. Sci*. **1987**, *185*, 450.